

Removal of Toxic Heavy Metals Lead and Mercury from Aqueous Medium by Adsorption onto Acid Functionalized-Nanoporous Carbon/MnO₂ Nano Composite

ShahinPathan^{#1}, Nancy Pandita^{*2}

[#]Assistant Professor, Department of Basic Sciences and Humanities, K. J. Somaiya Institute of Engineering and Information Technology, Sion (E), Mumbai-400022, India

^{*}Department of Chemical Sciences, Sunandan Divatia School of Science, NMIMS University, Vile Parle (West), Mumbai-400056, India

Abstract

Acid functionalized-Nanoporous carbon/MnO₂ nanocomposite was prepared from grass clippings as carbon precursor and used for removal of Pb(II) and Hg(II) from aqueous medium. The adsorption study of Pb(II) and Hg(II) on the surface of Af-NPC/MnO₂ was carried out with respect to factors such as pH, contact time and initial concentration. The kinetic study shows that the process of removal of these metal ions follow pseudo second order kinetics and the experimental equilibrium data fitted better in Langmuir isotherm model with maximum monolayer adsorption capacities of 117.64 mg/g and 90.09 mg/g for Pb(II) and Hg(II) respectively. The process of adsorption was found to be very fast compared to other adsorbents from literature. The mechanism of adsorption is also proposed based on experimental results. The results of this study indicated that Af-NPC/MnO₂ is an efficient adsorbent for removal of both Pb(II) and Hg(II) from aqueous medium. It was also observed that the composite was more selective for Pb(II) comparing to Hg(II) in a binary mixture.

Key words – Composite, Kinetic study, Adsorption, heavy metals

I. INTRODUCTION

Rapid urbanization and technological developments have greatly increased probabilities of contamination of water by toxic heavy metals like lead and mercury. Both these toxic heavy metals occupy positions just below arsenic in the Priority list of hazardous substances compiled by US EPA and ATSDR. Wide spread use of lead in industries like battery manufacturing, mining, plating, ceramic and glass is responsible for increased levels of lead in water bodies. Hence European Union Restriction of Hazardous Substances Directive (RoHS 1, 2003) restricted use of materials containing Pb(II), Hg(II) and Cr(VI) in the production of various types of electronic and electrical equipment [1]. Lead contamination of drinking water is mainly due to contact of water with lead containing piping, fittings

of the water distribution system or plumbing. Main sources of mercury contamination are municipal waste, mercury bulbs, electrical equipment etc. Lead and mercury both are potent neurotoxins and accumulates in body, damaging the nervous system and causing brain disorders [2]. Due to severe toxicity, Bureau of Indian standards and US EPA has kept 0.01 mg/L and 0.001 mg/L as permissible limit in drinking water for Pb(II) and Hg(II) respectively, hence these toxic heavy metals must be removed from water.

Membrane filtration, chemical precipitation, oxidation-reduction, coagulation, ion exchange and adsorption onto suitable sorbents are few techniques commonly used for removal of these toxic heavy metals from water. Among all these techniques removal of toxic heavy metals from water is best achieved by adsorption onto suitable sorbents. Adsorbents such as resin [3], biomass [4], agricultural waste [5], carbon nanotubes [6], nanocomposites [7] and silica materials have been reported in literature for removal of these toxic heavy metals from water. Acid functionalized nanoporous carbon/MnO₂ (Af-NPC/MnO₂) nanocomposite was found efficient in removal of arsenic from water through process of adsorption in previous work reported [8]. Hence the same composite Af-NPC/MnO₂ was further analyzed for removal of Pb(II) and Hg(II) from aqueous medium in the present work.

II. EXPERIMENTAL DETAILS

A. Synthesis of Af-NPC/ MnO₂ nanocomposite

Af-NPC/MnO₂ nanocomposite was synthesized from grass clippings as described earlier [8, 9]. In brief Af-NPC was first synthesized by pyrolysis of grass in a tube furnace. Further in order to prepare Af-NPC/MnO₂ nanocomposite, Af-NPC was sonicated in deionized water for 15 min at room temperature. Then to this solution Mn (II) chloride solution was added with continuous stirring. After this 0.13M KMnO₄ solution was added drop wise under continuous stirring. The solution turned dark

brown indicating precipitation of MnO_2 on the surface of Af-NPC. This suspension was further heated to 80°C for 1h. Af-NPC/ MnO_2 composite was then filtered and washed repeatedly with deionized water and dried at 105°C .

B. Physicochemical characterization

Surface properties of Af-NPC/ MnO_2 were determined by X-ray photoelectron spectroscopy on Kratos Analytical, Axis Supra. All samples were dried in vacuum at room temperature before XPS analysis. Fourier Transform Infrared Spectroscopy (FTIR) analysis of nanocomposite was carried out before and after adsorption of toxic metals using Jasco, FTIR 460 Plus spectrometer with TGS detector, and the spectra were recorded between 4000 cm^{-1} to 400 cm^{-1} . For FTIR analysis Af-NPC/ MnO_2 composite was treated with 60 mg/L of each Pb(II) and Hg(II) aqueous solutions separately for 1 h at pH 5. After adsorption composite was filtered and dried at 100°C before FTIR analysis.

C. Adsorption Experiments

All chemicals used in the experiments were of analytical grades. Pb(II) and Hg(II) stock solutions of 1000 mg/L were prepared by mixing appropriate amounts of AR grade lead chloride and mercuric chloride in deionized water. Working solutions of desired metal ion concentrations were freshly prepared by diluting stock solutions. Adsorption experiments were carried out in batch mode in Erlenmeyer flask.

For the pH dependent removal efficiency the adsorption experiments were conducted by mixing 10 mL of 5 mg/L solution of each metal separately at different pH (2–12) range with 0.5 g/L of Af-NPC/ MnO_2 for about 1 h at 150 rpm and room temperature. Af-NPC/ MnO_2 was further analyzed in detail with respect to time, initial concentration and selectivity. In order to examine the adsorption kinetics, batch adsorption experiments were carried out by mixing 0.5 g/L Af-NPC/ MnO_2 to 10 ml of metal ion solutions with different concentrations (10, 20 and 30 mg/L) for predetermined time intervals (5, 10, 15, 20, 30, 60 and 120 min) at pH 5 separately. The adsorption of these metals for different initial concentrations (2–60mg/L) was investigated on Af-NPC/ MnO_2 at room temperature under the same optimum conditions. To study the selectivity of Af-NPC/ MnO_2 removal efficiency was also investigated in a binary system of Pb-Hg by increasing the concentration of each element from 1–20 mg/L keeping other parameters constant. All the samples after adsorption were filtered through $0.45\ \mu\text{m}$ syringe filters. Initial and final concentrations were determined by inductively coupled plasma-atomic emission spectrometer (ICP-AES, ARCOS from M/s. Spectro, Germany).

The recycling capacity of Af-NPC/ MnO_2 was investigated by performing three successive cycles of

adsorption-desorption. In the desorption process, 35 mg of used Af-NPC/ MnO_2 composite was dispersed into 10ml of 0.1N HCl and rotated on shaker for 20 min. All the samples were filtered and thoroughly washed several times with deionized water after each cycle of desorption and the composites were reused for adsorption in the next cycles. The initial metal ion concentration used to study adsorption desorption cycles was 10 mg/L.

All the adsorption experiments were performed in triplicates and the average values are reported here. The percentage removal efficiency (% R) and equilibrium arsenic adsorption capacity q_e (mg/g) were calculated by equations (1) and (2) respectively as under.

$$\%R = \frac{C_0 - C_e}{C_0} \times 100 \quad (1)$$

Error! Reference source not found.

$$q_e = \frac{(C_0 - C_e)V}{M} \quad (2)$$

Where C_0 and C_e are the initial and final equilibrium concentrations of arsenic ions (mg/L) in aqueous solution, V is the total volume of solution (L) and M is the adsorbent mass (g).

III. RESULTS AND DISCUSSION

A. Effect of pH

The adsorption capacity of nanocomposite for both Pb(II) and Hg(II) increases with increase in pH and maximum removal was seen at $\text{pH} \geq 5$ (Fig. 1). Hence further study was done at an optimum pH of 5. Below pH 7 Pb(II) predominantly exist as Pb^{2+} in water and above pH 7 Pb(II) precipitates as $\text{Pb}(\text{OH})_2$ [10]. As pH_{pzc} of Af-NPC/ MnO_2 was 3.5, adsorption of Pb was less at lower pH due to repulsion between Pb^{2+} ions and the positive surface of Af-NPC/ MnO_2 and increases above pH 3.5 due to electrostatic interaction between Pb^{2+} and negative surface of composite. Beyond pH 7 adsorption of lead was mainly due to precipitations of $\text{Pb}(\text{OH})_2$. In surface waters HgCl_2 predominates at lower pH and $\text{Hg}(\text{OH})_2$ predominates at higher pH ($\text{pH} < 7.0$) [7]. Hence the sorption of Hg(II) on the surface of composite increases with increase in pH due to complex formation of mercuric hydroxide with oxygen containing functional groups of composites.

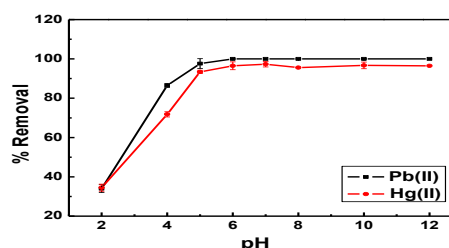


Fig 1: Effect of pH on adsorption of Pb(II) and Hg(II) on Af-NPC/MnO₂ (C₀= 5 mg/L)

B. Sorption kinetic studies

Sorption kinetic data was analyzed by Lagergren pseudo first-order model and Ho's pseudo-second-order reaction rate models, mathematical representations of these models are given in equations (3) and (4) respectively [8].

Lagergren pseudo first- order model

$$\frac{dq_t}{dt} = k_1(q_e - q_t) \tag{3}$$

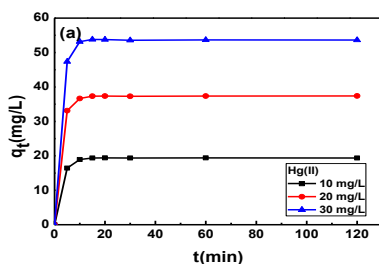
Ho's pseudo-second-order equation

$$\frac{dq_t}{dt} = k_2(q_e - q_t)^2 \tag{4}$$

Where q_t is amount of adsorbate in mg/g sorbed on the sorbent surface at any time t . k_1 and k_2 are the first order rate constant (min^{-1}) and the second-order rate constant (g/mg min) of sorption respectively and t is the time (min). The initial adsorption rate (h) at t Kinetic plots of Pb(II) and Hg(II) are represented in Fig. 2 and 3 respectively. Table 1 gives kinetic parameters calculated from plots. The initial adsorption rate (h) at $t = 0$ can also be calculated from

The pseudo second order model fitted well for both Pb(II) and Hg(II) adsorption as regression coefficients are higher than first order kinetics and q_e values are close to the experimental values. Pseudo second order kinetics implicate that the adsorption of Pb(II) and Hg(II) was taking place through chemisorptions on the surface of Af-NPC/MnO₂ and active functional groups present on the surface were the t/q_t vs t plot, using following equation (5).

$$h = K_2 q_e^2 \tag{5}$$



involved in the process. The equilibrium for adsorption was reached within 10 min.

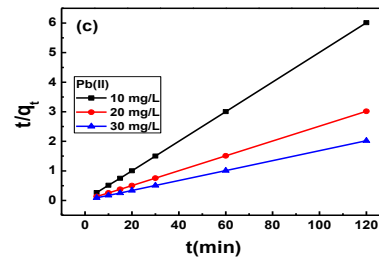
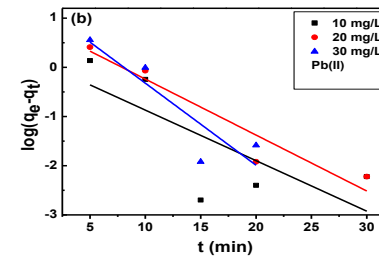
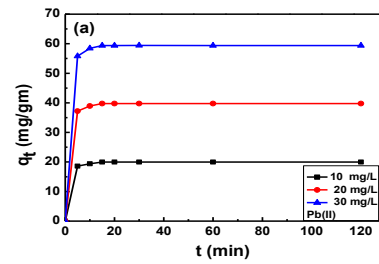
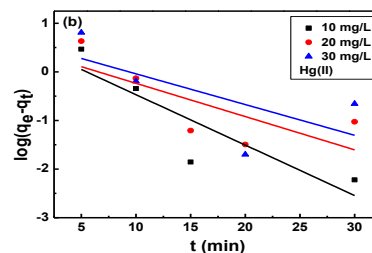


Fig 2: (a) Time profile of Pb(II) adsorption on Af-NPC/MnO₂ for different metal ion concentration (b) The pseudo first order kinetics model and (c) The pseudo-second-order kinetics model for adsorption of Pb(II) on Af-NPC/MnO₂ (C₀ = 10, 20 and 30 mg/L)



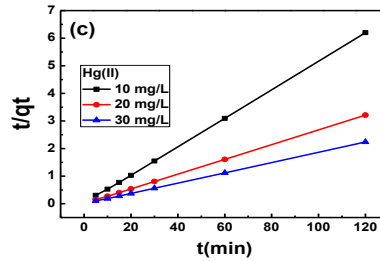


Fig 3: (a) Time profile of Hg(II) adsorption on Af-NPC /MnO₂ for different metal ion concentration (b) The pseudo first order kinetics model and (c) The pseudo-second-order kinetics model for adsorption of Hg(II) on Af-NPC/MnO₂ (C_o = 10, 20 and 30 mg/L)

m

Elements	C _o (mg/L)	Pseudo first order rate Parameters			Pseudo Second order rate Parameters			
		q _e (mg/g)	k ₁ (min ⁻¹)	R ²	q _e (mg/g)	k ₂ (g/mg min)	h (mg/g min)	R ²
Pb(II)	10	1.44	0.235	0.557	20	0.308	123.45	0.999
	20	7.88	0.26	0.919	39.84	0.169	270.27	0.999
	30	22.13	0.382	0.803	59.52	0.134	476.19	0.999
Hg(II)	10	3.69	0.237	0.782	19.41	0.193	72.99	0.999
	20	2.80	0.156	0.562	37.45	0.109	153.84	0.999
	30	5.16	0.110	0.733	53.76	0.108	312.5	0.999

C. Adsorption isotherms

Adsorption isotherms analysis was done using Langmuir, Freundlich and Dubinin–Radushkevich models.

1) Langmuir-Freundlich model

Langmuir isotherms imply that the adsorbent surface is homogeneous with equal adsorption affinity sites, while Freundlich isotherm model assumes the presence of heterogeneous adsorption sites. The linear form of Langmuir isotherms is given by following equation (6).

$$\frac{C_e}{q_e} = \frac{C_e}{q_m} + \frac{1}{K_L q_m} \tag{6}$$

Where K_L and q_m are the Langmuir adsorption constant (L/mg) and maximum monolayer adsorption capacity (mg/g) respectively. K_L represents affinity between solute and adsorbent. Another constant called as separation factor R_L was calculated by following equation where C_{omax} is maximum initial concentration.

$$R_L = (1/1+K_L C_{omax}) \tag{7}$$

The linear form of the Freundlich isotherm model is described by equation (8).

$$\log q_e = \log K_F + \frac{1}{n} \log C_e \tag{8}$$

Where K_F is Freundlich constant which is measure of adsorption capacity in mg/g and n is adsorption intensity respectively. The bond energy increases proportionally with surface density as n is more than one. Fig 4 shows Langmuir-Freundlich

isotherm plots and Table 2 gives different parameters calculated from the slope and intercepts of two isotherms plots. Both the adsorption models fitted well for adsorption of these toxic elements. Langmuir model fitted better to the adsorption as reflected by high value of correlation coefficient, suggesting monolayer adsorption of Pb(II) and Hg(II) on the surface of Af-NPC/MnO₂ and that there is no interaction among adsorbed ions. Freundlich constant n was found to be 3 and 2 for Pb(II) and Hg(II) respectively which implies that adsorption of both Pb(II) and Hg(II) was favourable on the surface of Af-NPC/MnO₂ and bond energy also increases proportionally with surface density as n is more than

1. The maximum adsorption capacities by Langmuir model were 117.64 mg/L and 90.09 mg/L for Pb(II) and Hg(II) respectively with initial concentration of 60 mg/L. The values of Separation factor R_L 0.084 and 0.024 implies that Langmuir isotherm is favorable ($0 < R_L < 1$). Hence based on isotherm study

we can conclude that Af-NPC/MnO₂ could be an efficient adsorbent for removal of both Pb(II) and Hg(II) due to good affinity and adsorption capacity.

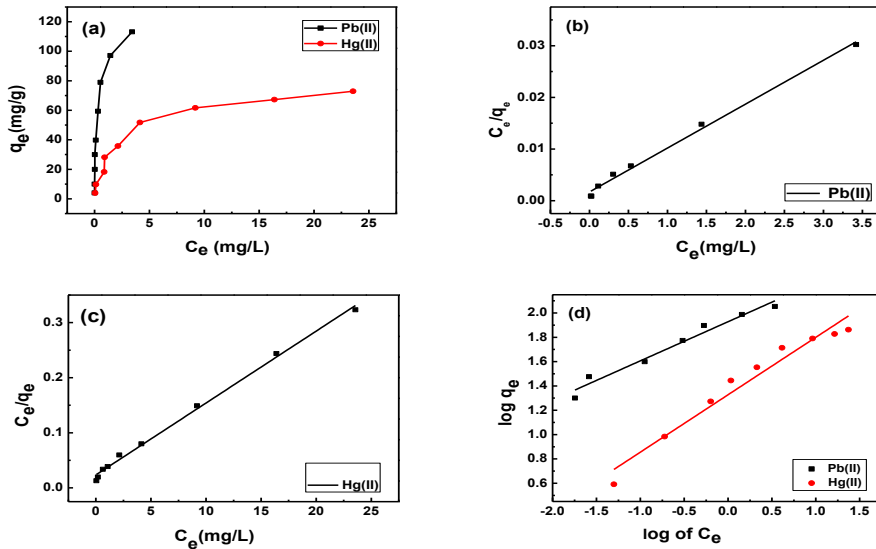


Fig 4. (a) Adsorption isotherm of Pb(II) and Hg(II) (b) and (c) Langmuir (d) Freundlich isotherm graphs of Pb(II) and Hg(II) adsorption on Af-NPC/MnO₂ at room temperature ($C_o = 2-60$ mg/L)

Table 2. Langmuir and Freundlich isotherm parameters for sorption of Pb(II) and Hg(II) on the surface of Af-NPC/MnO₂ at room temperature

Elements	Langmuir				Freundlich		
	q_m (mg/g)	K_L (L/mg)	R_L	R^2	K_F (mg/g)	n	R^2
Pb(II)	117.64	6.6	0.084	0.994	1.982	3	0.97
Hg(II)	90.09	5	0.024	0.996	1.427	2	0.949

2) **Dubinin-Radushkevich model (D-R)**

D-R model was used to determine nature of adsorption. The D-R model is represented by following equation [7].

$$\ln q_e = \ln q_m - \beta \epsilon^2 \tag{9}$$

Where β ($\text{mol}^2 \text{KJ}^{-2}$) is a constant related to mean adsorption energy and ϵ is the Polanyi potential which can be calculated from the following equation.

$$\epsilon = RT \ln \left(1 + \frac{1}{C_e} \right) \tag{10}$$

Where T is the absolute temperature in Kelvin and R is the universal gas constant ($8.314 \text{ Jmol}^{-1}\text{K}^{-1}$).

C_e is concentration of arsenic ions at equilibrium in aqueous medium. The slope of plot of $\ln q_e$ versus ϵ^2 gives β ($\text{mol}^2 \text{KJ}^{-2}$) and the intercept yields the sorption capacity q_m (mg/g). The sorption energy or mean free energy E can also be calculated by using following relationship.

Error! Reference source not found.
$$\tag{11}$$

The value of mean free energy helps in understanding nature of bonding between adsorbate and adsorbent. Value of E less than 8 kJ/mol indicates physical adsorption and value between 8-16 kJ/mol implies chemisorptions [7]. Fig 5 gives D-R model plots. The mean free energy calculated for Pb(II) and Hg(II) using equation (11) were 7 kJ/mol and 3.16

kJ/mol respectively. Since the values of E were less than 8 kJ/mol, adsorption of Pb(II) and Hg(II) was taking place through physical interaction on the surface of Af-NPC/MnO₂.

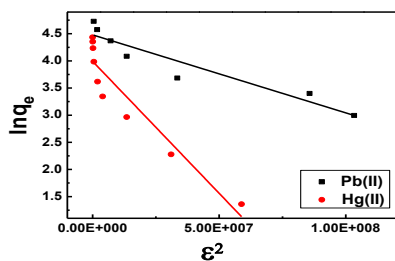


Fig 5: D-R plot for Pb(II) and Hg(II) adsorption on Af-NPC/MnO₂ at room temperature. (C₀ = 2-60 mg/L)

D. Selective adsorption of lead in binary system of Pb-Hg

Percentage removal of Hg(II) by Af-NPC/MnO₂ reduces from 94 % to 17 % in increasing concentration of Pb(II) from 1 to 20 mg/L. But no effect was observed on the removal efficiency of composite for Pb(II) in increasing concentration of Hg(II), hence Af-NPC/MnO₂ was found more selective for Pb(II) as represented in Fig 6. Lead interacts more strongly with negatively charged composite due to electrostatic interactions at pH 5 and competitively inhibits adsorption of Hg(II).

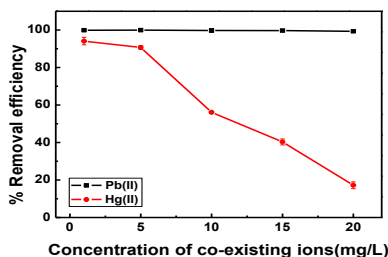


Fig 6: Effect of increasing ionic concentration (1-20 mg/L) in binary solution of Pb-Hg

F. Mechanism of adsorption

In order to understand the mechanism of adsorption XPS and FTIR analysis was carried out after adsorption of lead and mercury on the surface of Af-NPC/MnO₂.

1) XPS analysis

XPS wide spectra show presence of separate peaks for C1s, O1s, Mn2p, Pb4f and Hg4f in Fig. 8. As no major changes were observed after adsorption of Pb(II) and Hg(II) in different binding energies during the process of adsorption, new bonds did not form after adsorption. XPS results have shown Pb4f core levels at B.E 138 eV and 143 eV in Pb(II) adsorbed Af-NPC/MnO₂ [12]. Hg4f core levels were observed at B.E 101.2 eV and 105 eV in Hg(II) adsorbed Af-NPC/MnO₂ [13]. Presence of these

E. Sorbent regeneration

Percentage adsorption desorption efficiency of Af-NPC/MnO₂ for metal ions is represented in Fig. 7(a) and (b) for three consecutive cycles. It was observed that 0.1N HCL could elute 89-95% of adsorbed Pb(II) and Hg(II) from Af-NPC/MnO₂. The results of these studies showed that Af-NPC/MnO₂ has good re-use potential and even at the third cycle the sorption efficiency was reduced only by 2 %. From these results, it seems that Af-NPC/MnO₂ could be used as an effective alternative sorbent for removal of both Pb(II) and Hg(II). The ratio of volume of initially treated solution to the volume of 0.1N HCL solution used for desorption was 7.

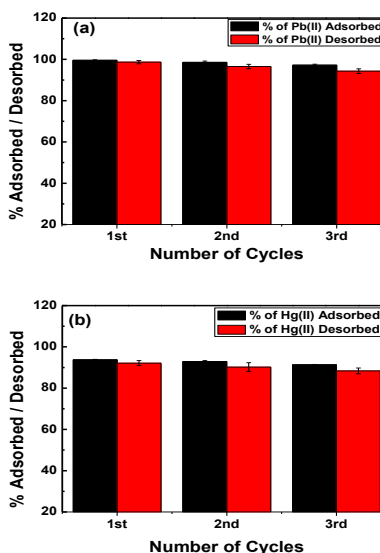


Fig 7: (a) and (b) % Adsorption / desorption efficiency of Af-NPC/MnO₂ for Pb(II) and Hg(II) respectively during three consecutive cycles. (C₀ = 10 mg/L)

peaks indicates existence of Pb(II) and Hg(II) on the surface of composite after adsorption from an aqueous medium.

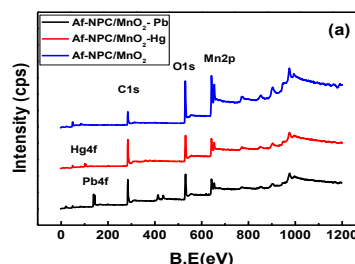


Fig 8: Wide XPS spectrum of Af-NPC/MnO₂

2) **FTIR analysis**

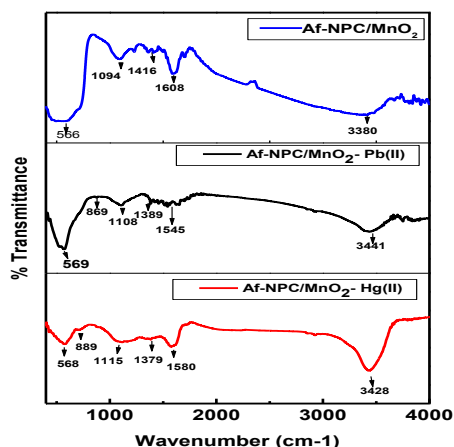


Fig 9. FTIR spectrum of Af-NPC/MnO₂ before and after adsorption of Pb(II) and Hg(II) from aqueous medium at pH 5

Fig 9 shows FTIR spectra of Af-NPC/MnO₂ before and after adsorption of Pb(II) and Hg(II). The shifts in vibrational frequencies of -C=O, -OH, and -COO groups were observed after adsorption of Pb(II) and Hg(II). This implies interaction of oxygen containing groups with metal ions during the process of adsorption on the surface of Af-NPC/MnO₂. Peaks at 869 cm⁻¹ and 889 cm⁻¹ were of Pb-O and Hg-O stretching frequencies. No major shifts were seen in vibrational frequency of -C=O, -OH, and -COO groups, which proves that the bonding of metal ions with Af-NPC/MnO₂ was not strong leading to fast regeneration.

3) **Probable mechanism**

As pseudo second order rate fitted well for adsorption, the mechanism of adsorption must be

chemisorptions, but the mean free energy from D-R adsorption model imply that the process of adsorption was physical. XPS and FTIR analysis also indicate weak bonding between metal ions and adsorbent surface through oxygen containing functional groups. Hence we can conclude from all these findings that physico-chemical interactions were involved during the process of adsorption of Pb²⁺ through weak electrostatic interactions and adsorption of Hg²⁺ through complex formation on the surface of Af-NPC/MnO₂ (Eq. no. 12 and 13).



4) **Comparison of Af-NPC/MnO₂ with other sorbents from literature**

Table 3 and 4 gives comparison of adsorption capacity of Af-NPC/MnO₂ with other adsorbents from literature. Af-NPC/MnO₂ composite has better adsorption capacity and fast removal rate as compared to other adsorbents mentioned in following tables for Pb(II) and Hg(II). Comparatively higher surface area could be the main factor responsible for higher removal efficiency of Af-NPC/MnO₂ for Pb(II) and Hg(II).

Table 3. Summary of comparison of adsorption properties of Af-NPC/MnO₂ with other adsorbents reported in the literature for removal of Pb(II)

Adsorbent	pH	Adsorption capacity (mg/g)	Co (mg/L)	Equilibrium Time (min)	Adsorbent dosage (g/L)	Surface area (m ² /g)	Ref.
Maize tassel activated carbon	5.5	37.31	50	>60min	1.2	250	[5]
MWCNTs-TAA	4.5	43	140	45	1		[6]
Mucor roxii biomass	5	74.6	100	360 min	5		[4]
MnO ₂ coated Betonite	6	58.88	-----	----	2	64	[14]
MnO ₂ /CNTs nanocomposite	5	78.74	60	120 min	0.5	275	[15]
Af-NPC/MnO ₂	5	117.64	60	5-10 min	0.5	633	Present work

Table 4. Summary of comparison of adsorption properties of Af-NPC/MnO₂ with other adsorbents reported in the literature for removal of Hg(II)

Adsorbent	pH	Adsorption capacity (mg/g)	Co (mg/L)	Equilibrium Time (min)	Adsorbent dosage (g/L)	Surface area (m ² /g)	Ref.
MnO ₂ /CNTs nanocomposite	7	58.82	50	80min	1	110.38	[7]
Functionalized mesoporous silica materials	3	64.5	300	---	---	---	[16]
Ionic liquid [A336][MTBA] immobilized PVA–alginate beads	5.8	49.89	50	Several hrs	2	----	[17]
Functionalized multi-walled carbon nanotube	6	84.66	100	-----	0.4	110	[18]
Adulsa (Justicia adhatoda) Leaves Powder	6	107.5	100	40min	1	----	[19]
Malt spent rootlets	5	50.4	200	>60 min	1	---	[20]
Acid Acrylic Resin	7	70.42	50	50 min	.2	----	[3]
Af-NPC/MnO ₂	5	90.09	60	10 min	0.5	633	Present work

VI. CONCLUSION

Af-NPC/MnO₂ was found to be an efficient adsorbent over a wide pH range of 5-12 for removal of both Pb(II) and Hg(II). Adsorption equilibrium was reached within 10 min. No residual Pb(II) was detected after treatment of water with initial concentration below 6 mg/L and Hg(II) below 2 mg/L. The maximum monolayer adsorption capacities were 117.64 mg/g and 90.09 mg/g for Pb(II) and Hg(II) respectively. Adsorption of Pb(II) was taking place through electrostatic interactions and that of Hg(II) through complex formation. Af-NPC/MnO₂ was more selective for Pb(II) when treated in a binary mixture. Adsorption capacity reduces only by 2% up to the third cycle of adsorption. Due to fast removal rate, high adsorption capacity and regeneration capacity, Af-NPC/MnO₂ could be a promising adsorbent for removal of lead and mercury from water.

ACKNOWLEDGMENT

Authors are grateful to SAIF, ESCA and INUP, IIT Bombay for providing instrumental facilities.

REFERENCES

- [1] The restriction of the use of certain hazardous substances in electrical and electronic equipment, O. J. L., 2003, 37, pp 19–23.
- [2] L. Patrick, "Lead toxicity, a review of the literature. Part 1: Exposure, evaluation and treatment," *Altrn. Med. Rev.* vol. 11, pp. 2-22, March 2006.
- [3] Chien-Wen Chen, Mu-Cheng Kuo, Jyh-Horng Wu, Ming-Shien Yen, Sing-You Lai, "Hybrid Organic-Inorganic Materials Comprising Zirconia, Silica, and Thiazole Dye by Sol-Gel Process," *International Journal of Applied Chemistry*, Volume 2 Issue 2, 2015.
- [3] C. Karthika and M. Sekar, "Removal of Hg (II) ions from aqueous solution by Acid Acrylic Resin A Study through Adsorption isotherms Analysis," *I. Res. J. Environment Sci.* vol. 1, pp. 34-41, August 2012.
- [4] S.S. Majumdar, S.K. Das, R. Chakravarty, T. Saha, T. S. Bandyopadhyay, A. K. Guha, "A study on lead adsorption by *Mucor rouxii* biomass," *Desalination*, vol. 251, pp. 96-102, 2010.
- [5] M. Moyo, L. Chikazaza, B. C. Nyamunda, U. Guyo, Adsorption Batch Studies on the Removal of Pb(II) Using Maize Tassel Based Activated Carbon," *J. Chem.* Article ID 508934, pp. 1-8, August 2013.
- [7] P.S.V.Shanmukhi, Dr.K.Chandramouli and Dr.P.V.S.Machiraju, "Investigative Study of Structural morphology of Polypropylene and BaCo₃ - Nanoparticle Composites", *International Journal of Material Science and Engineering*, Volume 2 Issue 3 2016.
- [6] M. S. Tehrani, P. A. Azar, P. E. Namin, S. M. Dehaghi, "Removal of Lead Ions from Wastewater Using Functionalized Multiwalled Carbon Nanotubes with Tris(2-Aminoethyl) Amine," *J. Environ. Prot.* vol. 4, pp. 529-536, June 2013.
- [7] K. M. Hamideh, P. Majid, "Experimental study on mercury ions removal from aqueous solution by MnO₂/CNTs nano composite adsorbent," *J. Ind. Eng. Chem.* vol. 21, pp 221-229, January 2015.
- [8] P. Shahin, P. Nancy, K. Nand, "Acid functionalized-nanoporous carbon/MnO₂ composite for removal of arsenic from aqueous medium," *Arab. J. Chem.*, in press, 2016.
- [9] P. Shahin, P. Nancy, "Nanoporous carbon synthesized from grass for removal and recovery of hexavalent chromium," *Carbon Lett.* vol. 20, pp. 10-18, October 2016.
- [10] Y. H. Li, Y. Zhu, Y. Zhao, D. Wu, Z. Luan, Different morphologies of carbon nanotubes effect on the lead removal from aqueous solution, *Diamond Relat. Mater.* vol.15, pp. 90–94, 2006.
- [11] L. Boszke, G. Głosińska, J. Siepak, Some Aspects of Speciation of Mercury in a Water Environment *Pol. J. Environ. Stud.* vol. 11, pp. 285-298, March 2002.
- [12] X.-Y. Yu, T. Luo, Y.-X. Zhang, Y. Jia, B.-J. Zhu, X.-C. Fu, J.-H. Liu, and X.-J. Huang, "Adsorption of Lead(II) on O₂-Plasma-Oxidized Multiwalled Carbon Nanotubes: Thermodynamics, Kinetics and Desorption," *Appl. Mater. Interfaces*, vol. 3, pp. 2585–2593, June 2011.
- [13] K.P. Lisha, S.M. Maliyekkal, T. Pradeep, "Manganese dioxide nanowhiskers: A potential adsorbent for the removal of Hg(II) from water," *Chem. Eng. J.* vol. 160, pp. 432–439, March 2010.
- [14] E. Erena, B. Afsinb, Y. Onalc, J. Hazard. Mater. "Removal of lead ions by acid activated and manganese oxide-coated bentonite," vol. 161, pp. 677–685, Jan 2009.

- [15] S. G. Wang, W. X Gong, X. W. Liu, Y. W. Yao, B. Y. Gao, Q. Y. Yue, "Removal of Pb(II) from aqueous solution by adsorption on to Manganese Oxide - coated carbon nano tubes," *Sep. Purif. Technol.* vol. 58, pp. 7-23, 2007.
- [16] L. Zhang, S. Goh, X. Hu, R. Crawford, A. Yu, Removal of aqueous toxic Hg(II) by functionalized mesoporous silica materials," *J. Chem. Technol. Biotechnol.* vol. 87, pp. 1473–1479, March 2012.
- [17] Y. Zhanga, D. Kogelnig, C. Morgenbesser, A. Stojanovic, F. Jirsa, I. Lichtscheidl-Schultze, R. Krachler, Y. Li, B.K. Keppler, Preparation and characterization of immobilized [A336][MTBA] in PVA–alginate gel beads as novel solid-phase extractants for an efficient recovery of Hg (II) from aqueous solutions," *J. Hazard. Mater.* vol. 196, pp. 201-209, November 2011.
- [18] H. Mojtaba, B. Nader, Y. Habibollah, L. Qin, "Adsorption of mercury ions from synthetic and real wastewater aqueous solution by functionalized multi-walled carbon nanotube with both amino and thiolated groups," *Chem. Eng. J.* vol. 237, pp. 217–228, 2014.
- [19] M. Aslam, S. Rais, M. Alam, A. Pugazhendi, "Adsorption of Hg(II) from Aqueous Solution Using Adulsa (*Justicia adhatoda*) Leaves Powder: Kinetic and Equilibrium Studies," *J. Chem.* Article ID 174807, July 2013.
- [20] V. A. Anagnostopoulos, I.D. Manariotis, H. K. Karapanagioti Karapanagioti, C.V. Chrysikopoulos, "Removal of mercury from aqueous solutions by malt spent rootlets," *Chem. Eng. J.* vol. 213, pp. 135–141, December 2012.